Kinetic Investigations on the Fading Reaction between MX and SDS at Concentrations Below and Above the Critical Micellar Concentration

Jiajun Zuo [a], Guanglei Liu [a], Ke Wang [a], Zhihang Wang [b, c*], Nong Wang [a*]

[a] School of Chemistry and Chemical Engineering, Lanzhou Jiaotong University, Lanzhou 730070, China
[b] School of Engineering, College of Science and Engineering, University of Derby, Markeaton Street, Derby DE2 23AW, United Kingdom
[c] Department of Materials Science and Metallurgy, University of Cambridge, 27 Charles Babbage Road, Cambridge, CB3 0FS, United Kingdom

Corresponding Authors:

Zhihang Wang – E-mail: z.wang@derby.ac.uk; Nong Wang – E-mail: wangnong07@163.com

Abstract Murexide (MX), the ammonium salt of purpuric acid, was found to significantly fade in the presence of sodium dodecyl sulfate (SDS) within 2 hours. Herein, the fading reaction kinetics data between MX and SDS at concentrations below and above the critical micellar concentration were studied using a UV-Visible spectrophotometer equipped with a temperature control system. By establishing a kinetic model and analysing the data, the influences of micelle and temperature on reaction orders and rate constants were determined. These results indicate that micelle formation can influence the reaction mechanism, lead to a decrease in reaction rate constants (k) and a shift in the partial order (β) from positive to negative. These results demonstrate that the formation of micelles have a substantial impact on the rate of the MX fading reaction, providing a new approach for studying the role of micelles in dye fading mechanisms.

Keywords: Kinetic; Murexide; Sodium Dodecyl Sulfonate; Critical Micellar Concentration; Micelle

Introduction

The interaction between dyes and surfactants plays a crucial role in various technical fields[1-3], including dyeing technology[4], the photography industry [5], ion detection [6], and pharmaceutical applications [7], and has attracted widespread global attention [8-15]. It is well-known that surfactants at low concentrations reduce surface tension and exhibit a range of interfacial phenomena, typically existing in dispersed ionic or monomolecular states. Upon reaching a certain concentration, surfactants undergo self-assembly into molecular aggregates—such as micelles, microemulsions, vesicles, or liquid crystals—which can influence chemical reactions through local concentration effects, electrostatic interactions, polarity shifts, orientation, and microviscosity [16]. The interactions between surfactants and dyes in solution may occur at the single-molecule (or ion) level or involve dye molecules with organized surfactant structures such as micelles, reverse micelles, vesicles, lipid bilayers, or multilayer films [17]. These interactions often lead to significant changes in dye solubility, absorption spectra, and dyeing behavior. Regardless of the interaction form, the binding or separation of dye and surfactant molecules is primarily governed by electrostatic forces [18], hydrogen bonding [19], van der Waals forces [20], hydrophobic interactions [21], and entropy-driven effects [22]. The strength and nature of these interactions depend on the specific ionic groups, polar functionalities, and hydrophobic segments of the surfactant and dye molecules, rendering the interaction mechanisms highly diverse and complex.

In the textile industry, dyes can become significant pollutants due to their high solubility in water, making their removal from wastewater a major challenge. Investigating the fading behavior of dyes in the presence of surfactants is therefore valuable for developing new and effective decontamination strategies[23]. Hence, gaining a comprehensive understanding of the dynamic interactions between dyes and micelles is essential. Samiey *et al.* studied the kinetics of the alkaline fading reaction of brilliant green in the presence of various surfactants, including Triton X-100, dodecyltrimethylammonium bromide (DTAB), and sodium dodecyl sulfate. They reported that the electrical charge of the brilliant green–surfactant complex significantly influenced the fading reaction rate[24]. Similarly, Somnath *et al.* investigated the alkaline hydrolysis rate of malachite green in the presence of cetyltrimethylammonium bromide (CTAB), finding that the reaction proceeded more rapidly in CTAB reverse micelles compared to continuous aqueous media or

conventional micelles—offering a more cost-effective method for malachite green removal from wastewater [25]. Sidra *et al.* demonstrated a reversal phenomenon in dye–surfactant systems, where the addition of an oppositely charged surfactant altered the electrostatic interactions and led to the dissociation of dye–surfactant aggregates [26]. Sharmin Akhter Maya et al. [27] explored the interaction between the anionic dye ethyl orange and cationic surfactants C_nTAC. Meanwhile, Manish Kumar Sah et al. [28] investigated the interaction between indigo carmine and N-alkyltrimethylammonium chloride. Furthermore, articles by Sharmin Akhter Maya et al. [29] have expanded the scope of research to include interactions between surfactants, drug molecules, and diol additives, revealing the potential applications of these interactions in enhancing dye performance, improving the sensitivity of analytical methods, and environmental monitoring [30,31]. In addition, various factors—such as the solvent used [32], salts concentration [33], temperature [34], pH [35], alcohol content [36,37], and other environmental conditions [38-43], can also significantly influence the interaction mechanisms between dyes and surfactants.

In several studies, surfactants have been regarded as reactants when examining their interactions with dyes [44,45]. However, other literature considers surfactants as catalysts; for instance, numerous studies have shown that surfactant micelles can exert a catalytic effect on the reaction [46]. In this study, the fading reaction of murexide (MX, a purple dye, Scheme 1) in aqueous solution was investigated in the presence of sodium dodecyl sulfate (SDS, Scheme 1). Assuming a 1:1 molar association between MX and SDS during the reaction, a kinetic model was established to describe the fading process. Based on this model, the rate constants and reaction order were determined. Furthermore, the influence of micelle formation on the reaction rate and the order of the association interaction was systematically analyzed. This work provides valuable insight into the kinetic behavior of dye–surfactant interactions, offering a foundation for the design of more efficient dye removal strategies in wastewater treatment and advancing the understanding of micelle-assisted reaction mechanisms.

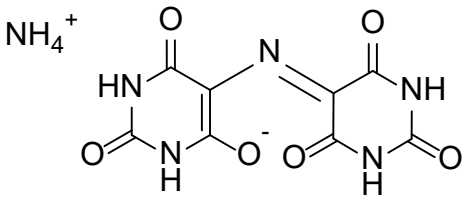

Murexide (MX)

Scheme 1 The molecular structure of murexide (MX), a purple dye.

Materials and methods

Materials

The dye MX (analytical grade, ≥99% purity) and surfactant SDS (analytical grade, ≥99% purity） were purchased from Shanghai Zhongqin Chemical Reagent Co., Ltd.

Methods

All absorption spectra were recorded using a UV-5200(PC) spectrophotometer with quartz cuvettes of 1 cm path length (Shanghai Yuanxi Instruments Co., Ltd.). A 100:1 molar ratio of SDS (5×10^{-2} mol dm^{-3}) to MX (5×10^{-4} mol dm^{-3}) was employed to ensure complete interaction. As shown in Figure 1, the addition of SDS to the aqueous MX solution resulted in a marked decrease in the intensity of MX's characteristic absorption band at 523 nm (from the black line to the red line). This change indicates the presence of an association interaction between MX and SDS. The significant alteration in maximum absorbance suggests that SDS strongly influences the electronic environment of the dye.

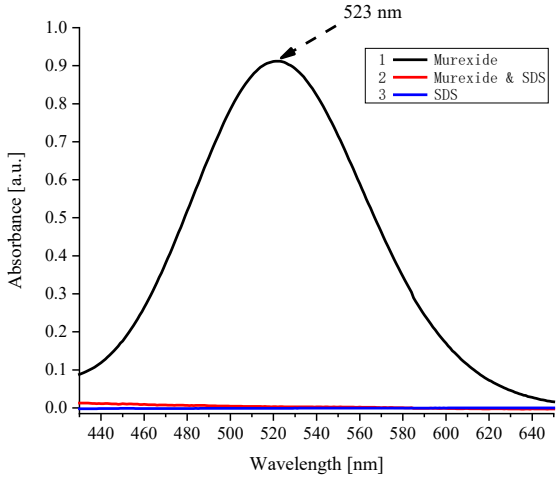

Figure 1. Absorption spectra: (1) MX in aqueous solution; (2) MX and SDS in aqueous solution; (3) SDS in aqueous solution, [SDS]= 5×10^{-2} mol dm^{-3}, [MX] = 5×10^{-4} mol dm^{-3}.

To further investigate the optimal molar ratio for dye fading between MX and SDS, two sets of experiments were then conducted by keeping the MX concentration constant at 5×10^{-4} mol dm^{-3} while varying the SDS concentration within the ranges of 1 ~ 5 $\times10^{-3}$ mol dm^{-3} and 5 ~ 7 $\times10^{-2}$ mol dm^{-3}, respectively. Much larger amount of substance SDS can remain the SDS concentration constant throughout the reaction, ensured pseudo-first-order reaction conditions, simplifying kinetic analysis. The 5 $\times10^{-2}$ mol dm^{-3} SDS concentration (~5 times of CMC) guaranteed the formation of micelle, enabling clear observation of micellar effects on reaction kinetics. All absorbance measurements were recorded within the range of 0.1 ~ 1 to minimize system errors. The concentration of MX during its fading reaction with SDS was determined by monitoring the solution's absorbance. A kinetic model was established to describe the influence of SDS on the reaction order and rate constant. Given that the critical micelle concentration (CMC) of SDS is reported to be 9.9 ~ 10.9×10^{-3} mol dm^{-3} in the literature [47-49], the fading reaction was then investigated at SDS concentrations both below and above the CMC.

Association reaction kinetics model

Assuming an association between MX and SDS, the equilibrium can be expressed by the following equation:

$$\mathrm{MX} + \mathrm{SDS} \rightarrow \mathrm{P}$$

The rate equation for the fading reaction between MX and SDS can be written as

$$r = -\frac{dc_{\mathrm{MX}}}{dt} = kc_{\mathrm{MX}}^{\alpha}c_{\mathrm{SDS}}^{\beta} \quad (1)$$

where t is the reaction time; r is the rate of fading reaction; c_{MX} and c_{SDS} are the concentrations of MX and SDS, respectively; k is reaction rate constants; α and β is the partial order of association reaction.

Assuming that the SDS concentration is much greater than that of MX ($c_{\mathrm{SDS}} >> c_{\mathrm{MX}}$), the concentration of SDS remains effectively constant throughout the reaction. Therefore, the rate equation simplifies to:

$$k' = kc_{\mathrm{SDS}}^{\beta} \quad (2)$$

where k' is the apparent reaction rate constant.

Substituting Eq. (2) into Eq. (1) gives:

$$r = -\frac{dc_{\mathrm{MX}}}{dt} \approx k' c_{\mathrm{MX}}^{\alpha} \tag{3}$$

Integration of Eq. (3) yields:

$$t = \frac{-1}{(-\alpha+1)k'} c_{\mathrm{MX}}^{-\alpha+1} + C \tag{4}$$

where C is the integration constant.

The actual absorbance A measured at 523 nm can then be expressed as:

$$A_{\mathrm{C}} = \varepsilon_{\mathrm{MX}} \left(c_{\mathrm{MX}}^{0} - c_{\mathrm{P}} \right) + \varepsilon_{\mathrm{P}} c_{\mathrm{P}} + \varepsilon_{\mathrm{SDS}} c_{\mathrm{SDS}} \tag{5}$$

Where $\varepsilon_{\mathrm{MX}}$, ε_{P} , and $\varepsilon_{\mathrm{SDS}}$ are the molar absorptivities of MX, the reaction product, and SDS, respectively.

As shown in Figure 1, $\varepsilon_{\mathrm{SDS}} \approx \varepsilon_{\mathrm{P}} \approx 0$, indicating their absorbances can be neglected. Therefore, Eq. (5) simplifies to:

$$A_{\mathrm{C}} = \varepsilon_{\mathrm{MX}} \left(c_{\mathrm{MX}}^{0} - c_{\mathrm{P}} \right) \tag{6}$$

The concentration of MX can then be expressed as:

$$c_{\mathrm{MX}} = c_{\mathrm{MX}}^{0} - c_{\mathrm{P}} \tag{7}$$

By replacing eq. (7) into eq. (6), yield the following equation:

$$c_{\mathrm{MX}} = \frac{A_{\mathrm{C}}}{\varepsilon_{\mathrm{MX}}} \tag{8}$$

Experimentally, after measuring A_C, the value of c_{MX} was calculated by eq. (8), and the reaction order α and apparent reaction rate constant k' at different temperature of this association process were fitted out by nonlinear fitting ($y = \frac{-1}{(-\alpha+1)k'} x^{-\alpha+1} + Constant$) of eq. (4). Then k at different temperature and β can later be obtained by nonlinear fitting from eq. (2).

Finally, according to the integral form of Arrhenius equation：

$$\ln k = -\frac{E_a}{RT} + \ln A \tag{9}$$

We can obtain the pre-exponential factor A and activation energy E_{a}.

Results and discussion

To eliminate experimental error caused by temperature variations, the molar absorption coefficient of MX at different temperatures was measured. As shown in

Figure 2, a series of aqueous MX solutions with concentrations ranging from 1 to 5×10^{-4} mol dm^{-3} was prepared, and their absorbance was recorded at various temperatures. Using the Lambert–Beer law and the data from Figure 2, the molar absorption coefficients at each temperature were calculated and are presented in Table 1. The results indicate that the molar absorption coefficient of MX decreases with increasing temperature. This trend can be attributed to the enhanced thermal motion of molecules at higher temperatures, which disrupts the electronic transition efficiency, leading to a reduction in the molar absorption coefficient.

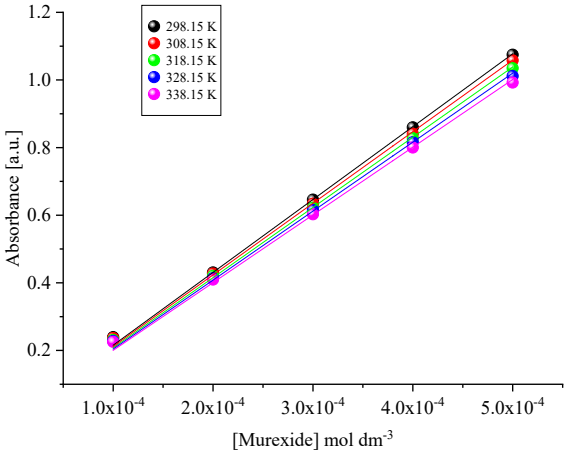

Figure 2. The absorbance of MX at 523 nm in aqueous solutions with varying concentrations and temperatures.

Table 1. Molar Absorption Coefficient of MX at Different Temperatures

T（K）	298.15	308.15	318.15	328.15	338.15
ε_{MX} （L·mol⁻¹·cm⁻¹）	2154.7±16.2	2117.5±17.4	2076.7±16.3	2040.3±17.7	2002.9±18.9

Below the CMC

The time–concentration profiles of MX at various SDS concentrations below the CMC and under different temperatures are shown in Figure 3. In all cases, the initial concentration of MX was fixed at 5×10^{-4} mol dm^{-3}.

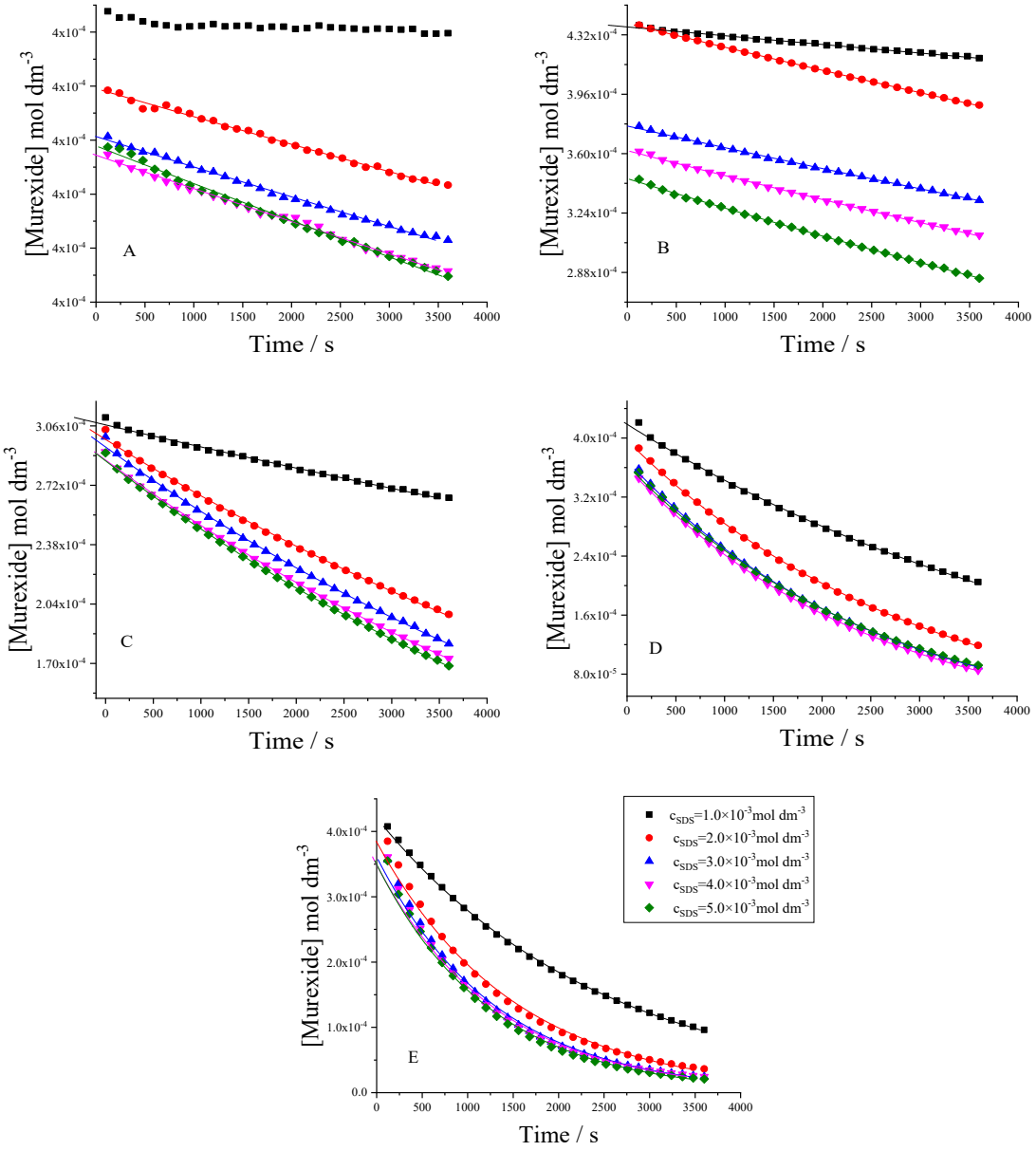

Figure 3. Time-dependent concentration profiles of MX after the addition of various SDS concentrations below the critical micelle concentration (CMC), measured at different temperatures. (A) 298.15 K; (B) 308.15 K; (C) 318.15 K; (D) 328.15 K; (E) 338.15 K. Dashed lines represent the experimental data, while solid lines indicate the corresponding fitting results.

As shown in Figure 3(A–E), higher temperatures resulted in a more rapid decrease in MX concentration over the same reaction time. The apparent reaction rate constants (k') were estimated by nonlinear regression within the temperature range of 298.15 ~ 338.15 K. This method provided reliable fitting results in most cases, with the exception of the first dataset, which failed to converge. The goodness of fit (R^2)

values from linear fitting using Equation (4) are listed in Table 2, all exceeding 0.99, confirming the reliability and accuracy of the kinetic parameters obtained.

Table 2 Goodness of Fit (R^2) from Linear Fitting Based on Equ (4)

T(K)	R^2				
298.15	----	0.9947	0.9966	0.9957	0.9950
308.15	0.9932	0.9998	0.9987	0.9990	0.9994
318.15	0.9976	0.9997	0.9998	0.9999	0.9999
328.15	0.9991	0.9999	0.9999	0.9999	0.9997
338.15	0.9997	0.9966	0.9972	0.9951	0.9969

The fitting results of kinetic parameters k' and α are summarized in Table 3. By fitting the data at different temperatures, yielded similar reaction order α, then we obtained the average value of α, which is 0.98 ± 0.03.

Table 3. Kinetic Parameters of the Reaction Below the CMC at Different Temperatures

T(k)	k_1'(s^{-1})	k_2'(s^{-1})	k_3'(s^{-1})	k_4'(s^{-1})	k_5'(s^{-1})	k(mM^{-1} s^{-1})	α	β
298.15	----------	2.28×10^{-7}	2.53×10^{-7}	2.80×10^{-7}	3.16×10^{-7}	3.70×10^{-6}		
308.15	2.16×10^{-7}	5.87×10^{-7}	6.18×10^{-7}	7.45×10^{-7}	9.26×10^{-7}	9.61×10^{-6}		
318.15	7.29×10^{-7}	1.99×10^{-6}	2.32×10^{-6}	2.43×10^{-6}	2.54×10^{-6}	5.00×10^{-5}	0.98	0.46
328.15	3.49×10^{-6}	5.81×10^{-6}	6.77×10^{-6}	6.93×10^{-6}	6.64×10^{-6}	8.85×10^{-5}		
338.15	7.14×10^{-6}	1.16×10^{-5}	1.32×10^{-5}	1.31×10^{-5}	1.38×10^{-5}	1.76×10^{-4}		

The β value to SDS and the rate constant k were obtained using Equations (2). As shown in Table 3 column 7 and 9. It can be found that k' increases with increasing SDS concentration at a given temperature, while k increases with rising temperature.

Since α = 0.98 is approximately equal to 1, Equation (4) is no longer applicable when assuming a first-order reaction. Therefore, a linear fitting approach was employed using the first-order rate law, which can be expressed as:

$$t = \frac{1}{k'} \ln \frac{c_{M,0}}{c_M} \tag{10}$$

or

$$\ln \frac{c_{M,0}}{c_M} = k't \tag{11}$$

The fitting results are shown in Figure 4, where the data points clearly follow a linear trend, indicating good agreement with the first-order kinetic model.

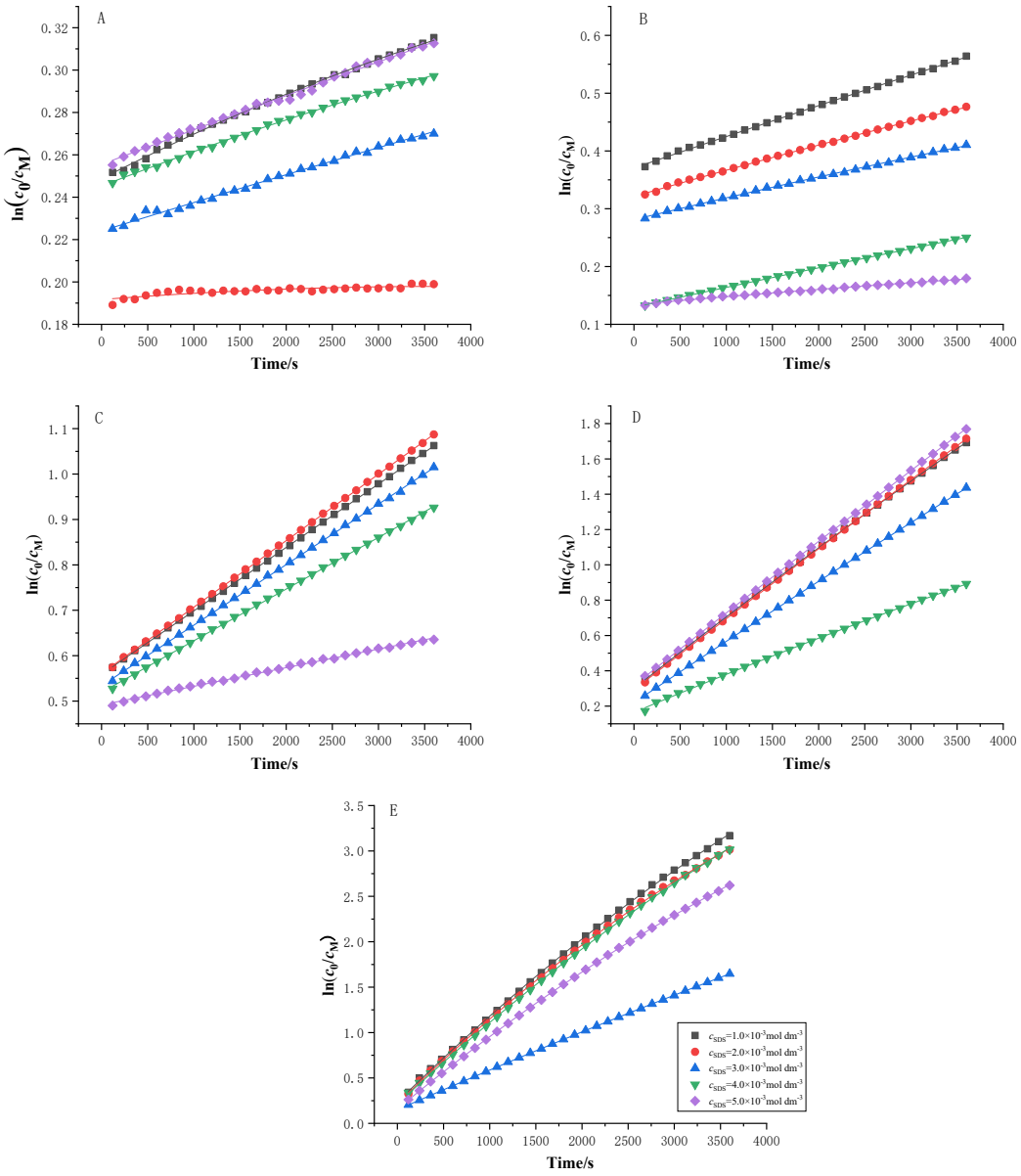

Figure 4. Plot of $\ln\frac{c_{M,0}}{c_M}$ against *t*. (A)298.15K; (B)308.15 K; (C)318.15 K; (D)328.15 K; (E) 338.15K.

Dashed lines represent the experimental data, while solid lines indicate the corresponding fitted results.

According to eq. (9), the integral form of Arrhenius equation, we obtained the pre-exponential factor A and activation energy E_a. As illustrated in Figure 5, the plot of ln$k$ versus $1/T$ yields a straight line. From the linear regression based on the Arrhenius equation, the apparent activation energy E_a and pre-exponential factor A were determined to be E_{a1} = 82.30 ± 2.02 kJ·mol^{-1} and A_1 = (9.70 ± 0.36) × 10^8 dm^3·mol^{-1}·s^{-1}, respectively.

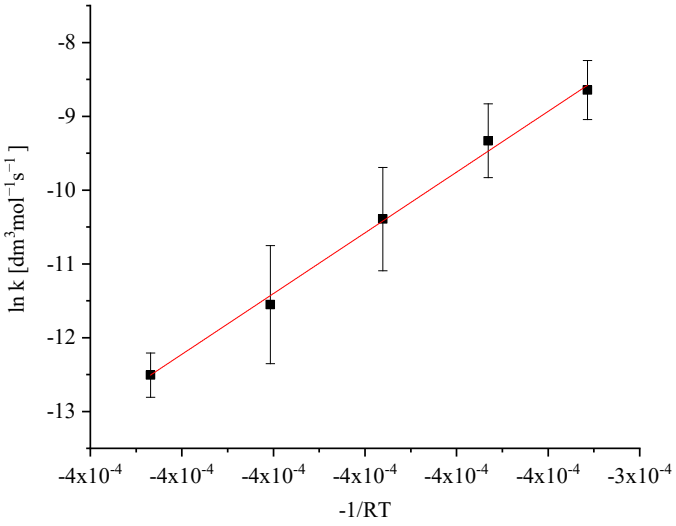

Figure 5. The plot of ln k *vs* $-\frac{1}{RT}$ below the CMC

Above the CMC

Similarly, the time-dependent concentration profiles of MX at various surfactant concentrations above the CMC of SDS under different temperatures are shown in Figure 6(A–E). After processing the kinetic data using the same method as before, a reaction order of $\alpha = 0.98 \pm 0.06$ with an R^2 of 0.99 was obtained, which is consistent with previous findings. All corresponding results are summarized in Table 4. Notably, the values of the rate constant k' decrease with increasing surfactant concentration at a given temperature, and the β values are negative, indicating an inhibitory effect of higher surfactant concentration on the reaction rate.

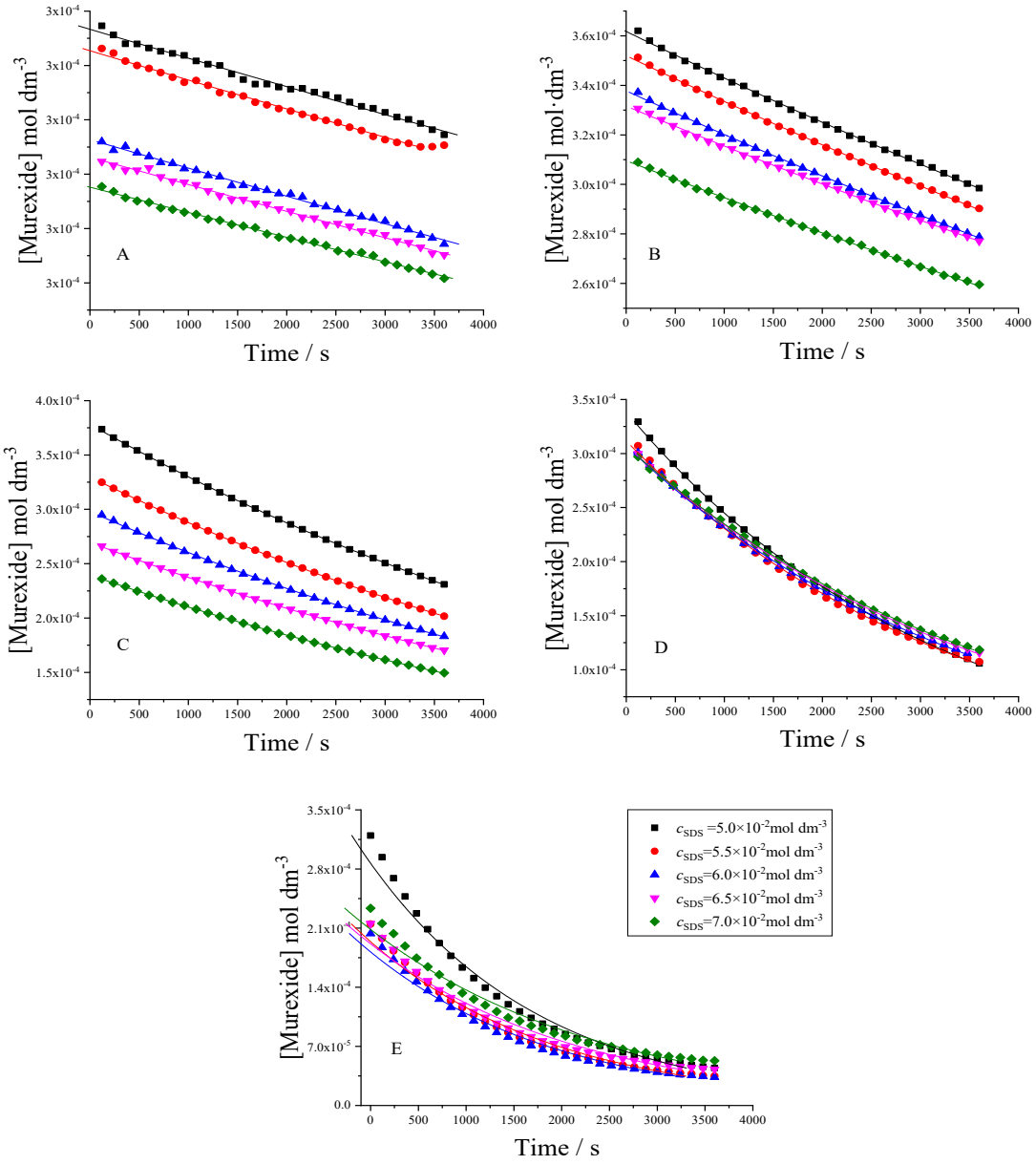

Figure 6. Time–concentration profiles of MX after the addition of various SDS concentrations above the critical micelle concentration (CMC) at different temperatures: (A) 298.15 K; (B) 308.15 K; (C) 318.15 K; (D) 328.15 K; (E) 338.15 K. Dashed lines represent experimental data, while solid lines indicate the corresponding fitting results.

Table 4. Kinetic Parameters of the Reaction Above the CMC at Different Temperatures.

T（K）	$k_1'(s^{-1})$	$k_2'(s^{-1})$	$k_3'(s^{-1})$	$k_4'(s^{-1})$	$k_5'(s^{-1})$	K（$dm^3 \cdot mol^{-1} \cdot s^{-1}$）	α	β
298.15	3.00×10^{-7}	2.93×10^{-7}	2.90×10^{-7}	2.85×10^{-7}	2.73×10^{-7}	8.77×10^{-8}		
308.15	9.30×10^{-7}	9.38×10^{-7}	9.32×10^{-6}	8.66×10^{-7}	8.59×10^{-7}	2.75×10^{-7}		
318.15	2.38×10^{-6}	2.37×10^{-6}	2.35×10^{-6}	2.21×10^{-6}	2.26×10^{-6}	7.03×10^{-7}	0.98	-0.42
328.15	5.61×10^{-6}	5.20×10^{-6}	4.90×10^{-6}	4.72×10^{-6}	4.62×10^{-6}	1.53×10^{-6}		
338.15	9.61×10^{-6}	8.80×10^{-6}	8.76×10^{-6}	7.85×10^{-6}	7.23×10^{-6}	2.58×10^{-6}		

As shown in Figure 7, the apparent activation energy (E_{a2}) and pre-exponential factor (A_2) for the reaction above the CMC were determined to be 74.37 ± 3.68 kJ·mol^{-1} and $(1.02 \pm 0.10) \times 10^6$ dm^3·mol^{-1}·s^{-1}, respectively. By comparing these values with those obtained below the CMC, the ratios E_{a1}/E_{a2} and A_1/A_2 were calculated to be 1.11 and 950.98, respectively. These results indicate that while the apparent activation energies before and after micelle formation are relatively similar, the pre-exponential factor below the CMC (A_1) is over 900 times greater than that above the CMC (A_2), suggesting a significant difference in the frequency or likelihood of successful collisions in the two environments.

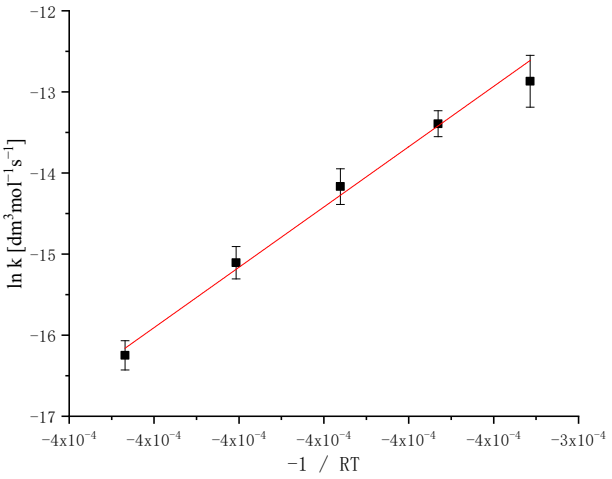

Figure 7. The plot of ln k vs $-\frac{1}{RT}$ above the CMC.

By comparing Tables 3 and 4, it can be observed that the values of α remain unchanged. However, the formation of micelles results in a noticeable decrease in the reaction rate constants k', while the value of β shifts from a positive value of 0.46 to a negative value of -0.42. Since β represents the reaction order with respect to SDS, this change indicates that micelle formation significantly influences the reaction dynamics.

According to collision theory, increasing the concentration of surfactant should enhance the collision frequency between dye molecules and surfactant molecules, thereby promoting the reaction. However, once micelles are formed, many dye molecules become encapsulated within micelles. This encapsulation restricts the free diffusion of the dye molecules, limiting their availability for effective collisions. Additionally, the outward-facing polar heads of SDS micelles hinder interactions

between dye molecules and the reactive sites, as the encapsulated dye can only collide with the non-polar tails of the SDS molecules—collisions that are generally ineffective in driving the reaction. Consequently, the presence of micelles leads to a reduction in the effective reaction rate and a reversal in the sign of β.

These findings suggest that the mechanism of the MX fading reaction differs notably before and after micelle formation, with micelles exerting a pronounced effect on the association and interaction mechanisms within the system.

Conclusions

Based on the association reaction kinetics model, the fading reaction between MX and the anionic surfactant SDS was investigated at surfactant concentrations both below and above the CMC. Integral kinetic curves and corresponding kinetic constants were obtained at different temperatures. Unlike previous studies that focused solely on single concentration regimes, we revealed distinct reaction mechanisms of MX fading reaction at SDS concentrations below and above the CMC: the formation of micelle caused the partial reaction order of SDS β shift from 0.46 to -0.42, while the rate constant k decreased from 3.70×10^{-3} $mM^{-1}\cdot s^{-1}$ to 8.77×10^{-5} $mM^{-1}\cdot s^{-1}$ at 298.15 K. Notably, the reaction order with respect to SDS (β) changed from positive to negative as the concentration crossed the CMC, and both the rate constant (k) and pre-exponential factor (A) decreased. These results indicate that micelle formation has a significant impact on the reaction rate, offering new insights into the role of micelles in the dye fading mechanism and suggesting a potential approach for further exploration of micelle-assisted reaction processes.

Acknowledgement

This work was supported by the Innovation Fund of Small and Medium-sized Enterprises of Gansu province (Grant No. 1407GCCA013), and the Gansu Province Key Research and Development Program (Grant No. 23YFGA0044).

Conflict of interest

The authors declare that they have no conflict of interest.

References

[1] J. Zheng, Z. Ma, Q. Zhang, L. Qiu, Z. Wang, N. Wang, ChemistrySelect **2024**, 9, e202400090.

[2] J. Sun, H. Wang, C. Zheng, G. Wang, Journal of Cleaner Production **2019**, 218, 284-293.

[3] J. Guo, Z. Wang, J. Jing, J. Tong, N. Wang, Journal of Dispersion Science and Technology **2017**, 39, 1208-1213.

[4] B. Li, W. Gong, X. Jing, B. Zheng, Journal of Dispersion Science and Technology **2020**, 42, 2043-2052.

[5] B. I. Shapiro, Russian Chemical Reviews **1994**, 63, 231.

[6] O. Prakash, S. Kumar, S. P. Mushran, Talanta **1979**, 26, 1167-1169.

[7] Berthois, Y., Katzenellenbogen, J., A., Katzenellenbogen, B., S., Proceedings of the National Academy of Sciences **1986**, 83, 2496-2500.

[8] H. Akbaş, Ç. Kartal, Dyes and Pigments **2007**, 72, 383-386.

[9] H. Akbas, C. Kartal, Spectrochim Acta A Mol Biomol Spectrosc **2006**, 65, 95-99.

[10] T. Shen, R. Xiao, Q. Wang, L. Yang, N. Wang, Journal of Dispersion Science and Technology **2014**, 35, 435-440.

[11] R. K. Dutta, S. N. Bhat, Bulletin of the Chemical Society of Japan **1993**, 66, 2457-2460.

[12] P. Forte-Tavčer, Dyes and Pigments **2004**, 63, 181-189.

[13] S. M. Ghoreishi, M. Behpour, A. G. Farsani, Dyes and Pigments **2007**, 74, 585-589.

[14] N. Wang, M. Zhao, Journal of Dispersion Science and Technology **2015**, 37, 190-195.

[15] R. T. Buwalda, J. Engberts, Langmuir **2001**, 17, 1054-1059.

[16] F. Warsi, M. R. Islam, M. A. Khan, M. Osama, M. Ali, Journal of Molecular Structure **2022**, 1260, 132798.

[17] Y. Wu, F. L. Yeh, F. Mao, E. R. Chapman, Biophysical Journal **2009**, 97, 101-109.

[18] D. C. Ghosh, P. K. Sen, B. Pal, International Journal of Chemical Kinetics **2021**, 53, 1228-1238.

[19] C. Fleischmann, M. Lievenbrück, H. Ritter, Polymers **2015**, 7, 717-746.

[20] C. Lim, D. S. Hwang, D. W. Lee, Carbohydrate Polymers **2021**, 259.

[21] B. Gohain, S. Sarma, R. K. Dutta, Journal of Molecular Liquids **2008**, 142, 130-135.

[22] K. Murakami, Dyes and Pigments **2002**, 53, 31-43.

[23] N. Aryanti, A. Nafiunisa, T. D. Kusworo, D. H. Wardhani, Membranes (Basel) **2020**, 10.

[24] Babak, SamieyMohammad, Rafi, Dargahi, Reaction Kinetics,Mechanisms&Catalysis **2010**, 101, 25-39.

[25] S. Dasmandal, H. K. Mandal, A. Kundu, A. Mahapatra, Journal of Molecular Liquids **2014**, 193, 123-131.

[26] S. T. Muntaha, M. N. Khan, Journal of Molecular Liquids **2014**, 197, 191-196.

[27] K. Edbey, M. Kumar, A. El-Hashani, H. Alarfi, D. Kumar, A. Bhattarai, J. Mol. Liq. **2024**, 407, 125166.

[28] M.K. Sah, K. Edbey, Z.O. Ettarhouni, A. Bhattarai, D. Kumar, *J. Mol. Liq.* **2024**, 399 , 124413.

[29] S. A. Maya, Alam, M. M. Alam, J. M. Khan, K. M. A. Haque, S.Rana, K. Hasan, M. Posa, D. Kumar, M. M. Rahman, M. A. Hoque,Colloids and Surfaces A: Physicochemical and Engineering Aspects, **2025**, 714, 136552.

[30] D. Kumar, J. M. Khan, N. Sultana, M. Posa, P. Sharma, B. Saha, A. Bhattarai,Chemical Physics, **2025**, 595, 112697.

[31] A. El-Hashani , M. K. Sah, K. Edbey, R. G. Ismael, D. Kumar, A. Bhattarai,Royal Society Open Science, **2025**, 12, 241344.

[32] B. Samiey, S. Ahmadi, Journal of Solution Chemistry **2012**, 42, 151-164.
[33] L. D. L. Miranda, C. R. Bellato, M. P. F. Fontes, M. F. de Almeida, J. L. Milagres, L. A. Minim, Chemical Engineering Journal **2014**, 254, 88-97.
[34] Babak, SamieySomayeh, Golestan, Central European Journal of Chemistry **2010**.
[35] L. Miranda, C. R. Bellato, M. Fontes, M. D. Almeida, J. L. Milagres, L. A. Minim, Chemical Engineering Journal **2014**, 254, 88-97.
[36] P. K. Behera, S. N. Panda, S. Sahu, Journal of Molecular Liquids **2013**, 177, 110-113.
[37] S. Mahbub, I. Shahriar, M. Iqfath, M. A. Hoque, M. A. Halim, M. A. Khan, M. A. Rub, A. M. Asiri, Journal of Environmental Chemical Engineering **2019**, 7, 103364.
[38] R. K. Dutta, S. N. Bhat, Bull.chem.soc.jpn **1992**, 65, 1089-1095.
[39] J. Yang, J Colloid Interface Sci **2004**, 274, 237-243.
[40] S. S. Shah, R. Ahmad, S. Shah, K. M. Asif, K. Naeem, Colloids & Surfaces A Physicochemical & Engineering Aspects **1998**, 137, 301-305.
[41] Y. Miyashita, S. Hayano, Bulletin of the Chemical Society of Japan **2006**, 54, 3249-3252.
[42] J. Fanzo, Global Food Security **2015**, 7, 15-23.
[43] S.-T. Muntaha, M. N. Khan, Physics and Chemistry of Liquids **2018**, 58, 8-17.
[44] M. F. Nazar, S. S. Shah, M. A. Khosa, Journal of Surfactants and Detergents **2010**, 13, 529-537.
[45] A. R. Tehrani-Bagha, R. G. Singh, K. Holmberg, Journal of Colloid and Interface Science **2012**, 376, 112-118.
[46] A. Raducan, A. Olteanu, M. Puiu, D. Oancea, Central European Journal of Chemistry **2008**, 6, 89-92.
[47] A. Jańczuk, M. L. González-Martin, J. M. Bruque, C. Dorado-Calasanz, J. M. D. Pozo, Journal of Colloid and Interface Science **1995**, 176, 352-357.
[48] S. Shirzad, R. Sadeghi, Fluid Phase Equilibria **2014**, 377, 1-8.
[49] R. Sadeghi, S. Shahabi, The Journal of Chemical Thermodynamics **2011**, 43, 1361-1370.

Table of Contents

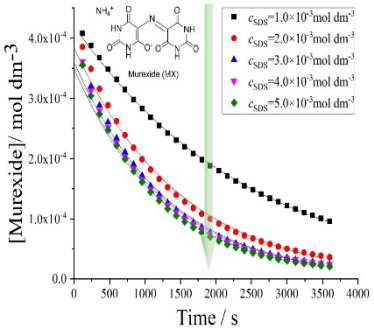

Murexide (MX), the ammonium salt of purpuric acid, was found to undergo significant fading in the presence of sodium dodecyl sulfate (SDS). By establishing a kinetic model and analysing the experimental data, the effects of micelle formation and temperature on the reaction order and rate constants were determined.